

Localization of Language Areas in Brain Tumor Patients by Functional Geometry Alignment

Georg Langs¹, Yanmei Tie², Laura Rigolo²,
Alexandra J. Golby², and Polina Golland¹

¹Massachusetts Institute of Technology,
Computer Science and Artificial Intelligence Lab,
{langs, polina}@csail.mit.edu

²Harvard Medical School, Department of Neurosurgery,
Brigham and Women’s Hospital,
{ytie, lrigolo, agolby}@bwh.harvard.edu

Abstract. The substantial reorganization of functional systems and hemodynamic changes caused by brain tumors make fMRI detection and characterization of functional brain regions in tumor patients a particularly difficult task. Our goal is to identify functional areas among different individuals and to localize potentially displaced active regions in patients. Localizing corresponding functional regions in patients with brain lesions is necessary for the pre-surgical localization of functional regions critical for language and other functions. In addition such findings may help to elucidate the mechanisms that control reorganization processes secondary to mass lesions in the brain. Anatomical data is only of limited value for this purpose. Rather than rely on spatial geometry, we propose to perform registration of functional regions between individuals in an alternative space whose geometry is governed by the functional interaction patterns in the brain. We first embed the brain into a functional map that reflects connectivity patterns during a task sequence. The resulting functional maps are then registered, and the obtained correspondences are propagated to the two brains. Initial experiments with the language system indicate that the proposed method yields improved correspondences across subjects. Our algorithm localizes language areas in tumor patients, even if the areas are not detected by standard approaches such as univariate regression.

1 Introduction

The detection of functional regions such as language networks in tumor patients is important for surgical planning and for studying the mechanisms that may displace functional cortex due to tumor growth. This localization is difficult, because a lesion may cause structural displacement, change hemodynamics, and can cause substantial reorganization of the functional areas. The standard fMRI analysis (such as the general linear model) faces challenges in localizing the activations; additional evidence for the location of the regions is needed. In this paper we propose to align neuroanatomy based on the functional geometry of fMRI signals during specific cognitive processes to match corresponding functional areas. For each subject, we construct a map by spectral embedding of the

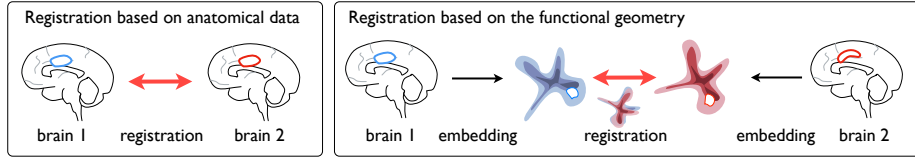


Fig. 1. Standard anatomical registration and the proposed functional geometry alignment. Functional geometry alignment matches the diffusion maps of fMRI signals of two subjects.

functional connectivity of the fMRI signals and register those maps to establish correspondences between functional areas in different subjects.

The primary clinical goal of the fMRI in this work is to localize language areas in tumor patients. The functional connectivity pattern for a specific area provides a refined representation of its activity. Our approach is to utilize the connectivity patterns to improve localization of the functional areas in tumor patients, by transferring the connectivity patterns from healthy subjects to tumor patients. The transferred patterns serve as a patient-specific prior for functional localization, improving the accuracy of detection. The functional geometry we use in this work is largely independent of the underlying anatomical organization. As a consequence, our method handles substantial changes in spatial arrangement of the functional areas that typically present significant challenges for anatomical registration methods.

Standard registration methods that match the anatomy of the brain between pairs or groups of individuals based on T1 weighted MRI data, such as the Talairach normalization [1] or non-rigid methods [2, 3] are of only limited usefulness in this context. Related work on functional registration of fMRI data either matches the centers of activated cortical areas [4, 5], or densely registers cortical surfaces [6, 7]. The fMRI signals at the surface points serve as a feature vector, and registration is performed by an elastic surface warp. These methods rely on a spatial reference frame for the registration, and use the functional characteristics as a feature vector of individual cortical surface points. This approach is limited in accuracy in cases of substantial reorganization of the functional structures (e.g., migration to the other hemisphere, or changes in topology of the functional maps). In contrast, our method of functional registration does not rely on spatial consistency.

We propose and demonstrate a functional registration method that operates in a space that reflects functional connectivity patterns of the brain. In this space, the connectivity structure is captured by a structured distribution of points, or *functional geometry*. Each point in the distribution represents a location in the brain and the relation of its fMRI signal to fMRI signals at other locations. Fig. 1 illustrates the method. To register functional regions among two individuals, we first embed both fMRI volumes independently, and then obtain correspondences by matching the two point distributions in the functional geometry. We argue that such a representation offers a more natural view of the co-activation patterns than the spatial structure augmented with functional feature vectors. The functional geometry can even handle long-range

reorganization, and topological variability in the functional organization of different individuals. It provides a prior for the detection of displaced functional regions in tumor patients. We evaluate the method on healthy control subjects and brain tumor patients who perform language mapping tasks. The language system is highly distributed across the cortex. The reorganization caused by tumor growth sometimes sustains language ability of the patient, even though the anatomy is severely changed. Preliminary results indicate that the proposed functional alignment outperforms anatomical registration in predicting activation in the target data. Furthermore, functional alignment is much less affected by the tumor presence than anatomical registration.

2 Methods

We first review the representation of the functional geometry that captures the co-activation patterns in a diffusion map [8, 9]. We then introduce a registration algorithm based on this representation.

2.1 Embedding the brain in a functional geometry

Given a fMRI sequence $\mathbf{I} \in \mathbb{R}^{T \times N}$ at N voxels, each carrying a BOLD signal over a time interval of T time points, we calculate the matrix $\mathbf{C} \in \mathbb{R}^{N \times N}$ that assigns each pair of voxels $\langle k, l \rangle$ a non-negative symmetric edge weight $c(k, l) = \exp(\frac{\text{corr}(\mathbf{I}_k, \mathbf{I}_l)}{\epsilon})$, where ϵ is the speed of weight decay. We define a graph whose vertices correspond to voxels and whose edge weights are determined by \mathbf{C} . In practice, we discard all edges with the weight below a chosen threshold and the corresponding Euclidean distance between the two voxels above another constant threshold to obtain a sparse graph.

We transform the graph into a Markov chain on the set of nodes by the normalized graph Laplacian construction [10]. The degree of each node $g(k) = \sum_l c(k, l)$ is used to define the directed edge weights of the Markov chain as $p(k, l) = \frac{c(k, l)}{g(k)}$, which can be interpreted as transition probabilities along the graph edges. It also defines a diffusion operator $Pf(x) = \sum p(x, y)f(y)$ on the graph vertices (voxels). The diffusion operator integrates all pairwise relations in the graph and defines a geometry on the entire set of BOLD signals. The graph is embedded in a Euclidean geometry by an eigenvalue decomposition of P [8]. The eigenvalue decomposition of the operator P results in a sequence of eigen values $\lambda_1, \lambda_2 \dots$ and corresponding eigen vectors Ψ_1, Ψ_2, \dots that satisfy $P\Psi_i = \lambda_i\Psi_i$ and constitute the so-called *diffusion map*: $\Psi_t \triangleq \langle \lambda_1^t \Psi_1 \dots \lambda_w^t \Psi_w \rangle^T$, where $w \leq T$ is the dimensionality of the representation, and t is a parameter that controls scaling of the axes in this newly defined space. $\Psi_t^k \in \mathbb{R}^w$ is the representation of voxel k in the functional geometry, and is comprised of the k th components of the first w eigenvectors. The global structure of the functional connectivity is reflected in the point distribution Ψ_t . The dimensions of the eigenspace are the directions that capture the highest amount of structure in the connectivity landscape of the graph.

The geometry is governed by the diffusion distance D_t on the graph: $D_t(k, l)$ is defined through the probability of traveling between two vertices k and l

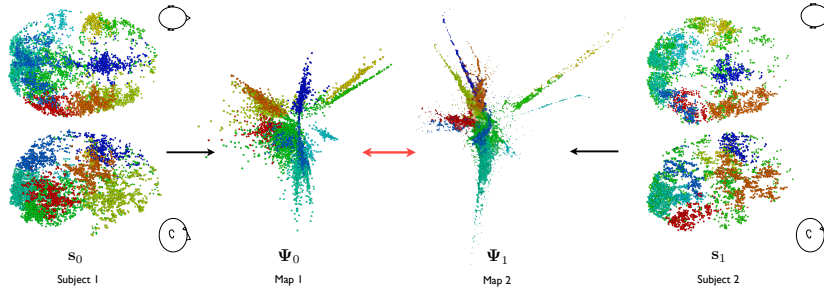


Fig. 2. Maps of two subjects in the process of registration: Left and right the axial and sagittal views of the points in the two brains are shown. The two central columns show plots of the first three dimensions of the embedding in the functional geometry after coarse rotational alignment. The colors indicate clusters which are only used for visualization.

taking all paths of at most t steps into account. It corresponds to the operator P^t parameterized by t - the diffusion time:

$$D_t(k, l) = \sum_{i=1, \dots, N} \frac{(p_t(k, i) - p_t(l, i))^2}{\pi(i)} \quad \text{where} \quad \pi(i) = \frac{g(i)}{\sum_u g(u)}. \quad (1)$$

The distance D_t is low if there is a large number of paths of length t with high transition probabilities between the nodes k and l .

The diffusion distance corresponds to the Euclidean distance in the embedding space: $\|\Psi_t(k) - \Psi_t(l)\| = D_t(k, l)$. The *functional* relations between fMRI signals are translated into spatial distances in the functional geometry. This particular embedding method is closely related to other spectral embedding approaches [11], but the parameter t offers the possibility to control the range of graph nodes that influence a certain local configuration. The embedding reflects the mutual diffusion distance between points, but is not unique up to rotation and the sign along individual coordinate axes. When computing the embedding, we flip the sign of each individual coordinate axis j so that $mean(\{\Psi_j(k)\}) - median(\{\Psi_j(k)\}) > 0, \forall j = 1, \dots, w$. Since the distributions typically have a long tail, and are centered at the origin, this step disambiguates the coordinate axis directions well. To facilitate notation, we assume the diffusion time t is fixed in the remainder of the paper, and omit it from the equations. The resulting maps are the basis for the functional registration of the fMRI volumes.

2.2 Functional Geometry Alignment

Let Ψ_0 , and Ψ_1 be the functional maps of two subjects. Ψ_0 , and Ψ_1 are point clouds embedded in a w -dimensional Euclidean space. Since the points in the maps correspond to voxels, registration of the maps establishes correspondences

between brain regions of the two subjects. At this point we do not know one-to-one correspondences of points in the two maps or of regions in the two volumes. However, the map is a structured point distribution, and we assume it allows for an unambiguous match between the two point clouds Ψ_0 and Ψ_1 . We initialize the registration with a coarse alignment of the two brains in the spatial coordinate framework. Based on these initial correspondences the maps are rotated so that the distance between a randomly chosen subset of points is minimized in the functional space. For the subsequent non-linear registration of the functional maps we employ the Coherent Point Drift algorithm [12]. We consider the points in Ψ_0 to be centroids of a Gaussian mixture model that are fitted to the points in Ψ_1 to minimize the energy

$$E(\chi) = - \sum_{k=1}^{N_1} \log \left(\sum_{l=1}^{N_2} e^{-\frac{1}{2} \frac{\|x_k^0 - x_l^1\|^2}{2\sigma^2}} \right) + \frac{\lambda}{2} \phi(\chi), \quad (2)$$

where ϕ is a function that regularizes the deformation χ of the point set.

Once the registration of the two distributions in the functional geometry is completed, we assign correspondences between points in Ψ_0 and Ψ_1 by a simple matching algorithm that for any point in one map chooses the closest point in the other map.

2.3 Evaluation

To validate the localization of the functional regions quantitatively we register pairs of subjects via the proposed functional geometry alignment, and the anatomical non-rigid demons registration [13, 14]. We restrict the computation to the grey matter. For computational reasons functional geometry embedding is performed on a random sampling of 8000 points excluding those that exhibit no activation (even with a liberal threshold of $p = 0.15$). We validate the accuracy of localizing activated regions in a target volume: (i) we measure the average correlation of the t-value maps (based on the standard General Linear Model [15]) between the source and the corresponding target regions after registration. A high value indicates that the aligned source t-maps have high predictive power for the target fMRI data - even if the target fMRI signal is below the activation threshold. (ii) We measure the overlap between regions in the target to which the activated source regions are mapped, and the activated regions in the target image.

To assess the relationship between the source and registered target regions relative to the fMRI activation, we measure the correlation between the BOLD signals in the activated regions of the source volume and the BOLD signals at the corresponding positions in the target volume. We are interested in two specific regions: (i) activated regions in the target image that were matched to activated regions in the source image, and (ii) non-activated regions in the target image that were matched to activated regions in the source image. The latter are of interest for the application of the method: they are candidates for activation identified by the functional alignment, even though they do not pass detection threshold in the target volume.

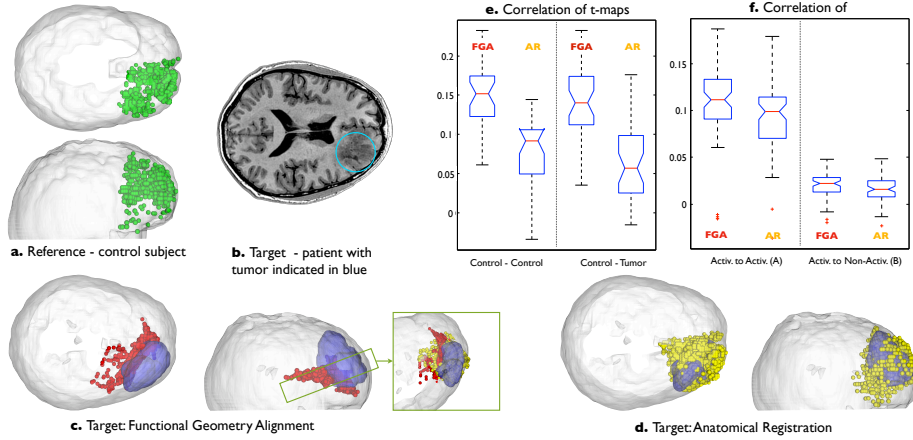


Fig. 3. Mapping a region by functional geometry alignment: a reference subject (a) aligned to a tumor patient (b). The green region in the healthy subject is mapped to the red region by the proposed functional alignment (c) and to the yellow region by anatomical registration (d). Note that the functional alignment places the region narrowly around the tumor location, while the anatomical registration result intersects with the tumor. Quantitative results show the correlation distribution of corresponding t-values after functional geometry alignment (FGA) and anatomical registration (AR) for control-control and control-tumor matches (e). The correlation of the BOLD signals for activated regions mapped to activated regions (left) and activated regions mapped to sub-threshold regions (right) is shown in (f).

3 Results

We demonstrate the method on a set of 6 control subjects and 3 patients with low-grade tumors in one of the regions associated with language processing. For all 9 subjects fMRI data was acquired using a 3T GE Signa system (TR=2000ms, TE=40ms, flip angle=90, slice gap=0mm, FOV=25.6cm, dimension $128 \times 128 \times 27$ voxels, voxel size of $2 \times 2 \times 4$ mm). The language task (antonym generation) block design was 5 min 10 sec, starting with a 10 sec pre-stimulus period. 8 task and 7 rest blocks each 20 sec. long alternated in the design. For each subject, anatomical T1 MRI data was acquired and registered to the functional data. We perform pair-wise registration in all 36 image pairs, 21 of which include at least one patient.

Fig.3 (a-d) illustrates the effect of a tumor in a language related region, and the corresponding registration results. An area of the brain associated with language is registered from a control subject to a patient with a tumor. The location of the tumor is shown in blue; the regions resulting from functional and anatomical registration are indicated in red, and yellow, respectively. While anatomical registration creates a large overlap between the mapped region and the tumor, functional geometry alignment maps the region to a plausible area narrowly surrounding the tumor.

Fig. 3 (e-f) reports quantitative comparison of functional alignment vs. anatomical registration. Functional geometry alignment achieves significantly higher correlation of t-values than anatomical registration (0.14 vs. 0.07, $p_i 10^{-17}$, paired

t-test, all image pairs). Anatomical registration performance drops significantly when registering a control subject and a tumor patient, compared to two control subjects (0.08 vs. 0.06, $p=0.007$). For functional geometry alignment the difference is not significant (0.15 vs. 0.14, $p=0.17$). Functional geometry alignment predicts 50% of the activated regions ($p < 0.05$, FDR corrected [16]) in the target brain, while anatomical registration predicts 29%.

These findings indicate that the functional alignment based matching of language regions among source and target subjects is affected less by the presence of a tumor than the matching by anatomical registration. Furthermore the functional alignment has better predictive power for the activated regions in the target subject.

For activated source regions mapped to activated target regions the average correlation between source and target BOLD is significantly higher for functional geometry alignment (0.108 vs. 0.097, $p=0.004$ paired t-test). For activated regions mapped to non-activated regions the same significant difference exists (0.020 vs. 0.016, $p=0.003$), but correlations are significantly lower. This significant difference between functional geometry alignment and anatomical registration vanishes for regions mapped from non-activated regions. The baseline of non-activated region pairs exhibits very low correlation (~ 0.003) and no difference between the two methods. Note that we evaluate the quality of functional registration based on correlation of the fMRI time courses in the matched region across subjects as opposed to the correlation of fMRI signals in the same subject that is used for functional connectivity calculation and forms the basis for the embedding.

We demonstrate that our alignment improves inter-subject correlation for activated source regions and their target regions, but not for the non-active source regions. This suggest that we enable localization of regions that would not be detected by the standard GLM analysis, but whose activations are similar to the source regions in the normal subjects.

4 Conclusion

In this paper we propose and demonstrate a method for registering neuroanatomy based on the functional geometry of fMRI signals. The method offers an alternative to anatomical registration; it relies on matching a spectral embedding of the functional connectivity patterns of two fMRI volumes. Initial results indicate that the structure in the diffusion map that reflects functional connectivity enables accurate matching of functional regions. When used to predict the activation in a target fMRI volume the proposed functional registration achieves higher predictive power than the anatomical registration. Moreover it is more robust to pathologies and the associated changes in the spatial organization of functional areas. The method offers advantages for the localization of activated but displaced regions in cases where tumor induced changes of the hemodynamics make direct localization difficult. In such cases the alignment can contribute evidence from healthy control subjects. Further research is necessary to evaluate the predictive power of the method for localization of specific functional areas.

5 Acknowledgements

This work was funded in part by the NSF IIS/CRCNS 0904625 grant, the NSF CAREER 0642971 grant, the NIH NCRR NAC P41-RR13218, NIH NIBIB NAGIC U54-EB005149, NIH U41RR019703, and NIH P01CA067165 grants, the Brain Science Foundation, and the Klarman Family Foundation.

References

1. Talairach, J., Tournoux, P.: Co-planar stereotaxic atlas of the human brain. Thieme New York (1988)
2. Fischl, B., Sereno, M., Tootell, R., Dale, A.: High-resolution intersubject averaging and a coordinate system for the cortical surface. *HBM* **8**(4) (1999) 272–284
3. Shen, D., Davatzikos, C.: HAMMER: hierarchical attribute matching mechanism for elastic registration. *IEEE Trans. Med. Imaging* **21**(11) (2002) 1421–1439
4. Thirion, B., Flandin, G., Pinel, P., Roche, A., Ciuciu, P., Poline, J.: Dealing with the shortcomings of spatial normalization: Multi-subject parcellation of fMRI datasets. *Human brain mapping* **27**(8) (2006) 678–693
5. Van Essen, D., Drury, H., Dickson, J., Harwell, J., Hanlon, D., Anderson, C.: An integrated software suite for surface-based analyses of cerebral cortex. *Journal of the American Medical Informatics Association* **8**(5) (2001) 443
6. Sabuncu, M., Singer, B., Conroy, B., Bryan, R., Ramadge, P., Haxby, J.: Function-based intersubject alignment of human cortical anatomy. *Cerebral Cortex* **20**(1) (2010) 130–140
7. Conroy, B., Singer, B., Haxby, J., Ramadge, P.: fmri-based inter-subject cortical alignment using functional connectivity. In: *Adv. in Neural Information Proc. Systems*. (2009) 378–386
8. Coifman, R.R., Lafon, S.: Diffusion maps. *App. Comp. Harm. An.* **21** (2006) 5–30
9. Langs, G., Samaras, D., Paragios, N., Honorio, J., Alia-Klein, N., Tomasi, D., Volkow, N.D., Goldstein, R.Z.: Task-specific functional brain geometry from model maps. In: *Proc. of MICCAI. Volume 11*. (2008) 925–933
10. Chung, F.R.: *Spectral Graph Theory*. American Mathematical Society (1997)
11. Qiu, H., Hancock, E.: Clustering and Embedding Using Commute Times. *IEEE TPAMI* **29**(11) (2007) 1873–1890
12. Myronenko, A., Song, X., Carreira-Perpinán, M.: Non-rigid point set registration: Coherent Point Drift. *Adv. in Neural Information Proc. Systems* **19** (2007) 1009
13. Thirion, J.: Image matching as a diffusion process: an analogy with Maxwell’s demons. *Medical Image Analysis* **2**(3) (1998) 243–260
14. Wang, H., Dong, L., O’Daniel, J., Mohan, R., Garden, A., Ang, K., Kuban, D., Bonnen, M., Chang, J., Cheung, R.: Validation of an accelerated ‘demons’ algorithm for deformable image registration in radiation therapy. *Physics in Medicine and Biology* **50**(12) (2005) 2887–2906
15. Friston, K., Holmes, A., Worsley, K., Poline, J., Frith, C., Frackowiak, R., et al.: Statistical parametric maps in functional imaging: a general linear approach. *Hum Brain Mapp* **2**(4) (1995) 189–210
16. Benjamini, Y., Hochberg, Y.: Controlling the false discovery rate: a practical and powerful approach to multiple testing. *Journal of the Royal Statistical Society. Series B (Methodological)* (1995) 289–300